HALL COEFFICIENT AND RESISTIVITY OF

AN AMORPHOUS PALLADIUM-SILICON ALLOY

Thesis by

Raymond Dean Ayers

In Partial Fulfillment of the Requirements

for the Degree of

Doctor of Philosophy

California Institute of Technology

Pasadena, California

1971

(Submitted May 26, 1971)

FOR SUE

ACKNOWLEDGMENT

iv.

ABSTRACT

The Hall coefficient and resistance in several specimens of an amorphous metallic alloy containing 80 at.% palladium and 20 at.% silicon have been investigated at temperatures between 4.2°K and room temperature. An ideal limiting behavior of these transport coefficients was analyzed on the basis of the nearly free electron model to yield a carrier density of 9×10^{22} cm.$^{-3}$, or about 1.7 electrons per palladium atom, and a mean free path of about $9\overset{\circ}{A}$ which is almost constant with temperature. The deviations of the individual specimens from this ideal behavior, which were small but noticeable in the relative resistivity and much greater in the Hall coefficient, can be explained by invoking disk-shaped crystalline regions with low resistivity and a positive Hall coefficient. A detailed calculation shows how a volume fraction of such crystalline material too small to be noticed in X-ray diffraction could have a significant effect on the resistivity and a much greater effect on the Hall coefficient.

v.

TABLE OF CONTENTS

I. INTRODUCTION

After the accidental discovery that gold-silicon alloys could be retained in a non-crystalline solid phase by rapid quenching [1], the first of several other such amorphous phases to be found by a systematic search was in the neighborhood of the very deep eutectic at 15.5 at.% Si in the system Pd-Si. [2] Because of the relative ease with which a successful quench could be obtained, the particular composition $Pd_{.8}Si_{.2}$ was singled out for intensive investigation by X-ray diffraction, electron microscopy and resistivity measurements. [3] The results of that work tended to confirm the belief that this really was a metallic system with only very short range order. The present investigation of the Hall coefficient in the same alloy was undertaken to see whether this transport coefficient could be interpreted in terms of the nearly free electron model (spherical Fermi surface, effective mass very near to the true mass of the electron) that has proved so useful in understanding electrical transport in liquid metals.

II. EXPERIMENTAL PROCEDURE

A. Preparation and testing of Hall effect specimens

The alloy containing 20 atomic percent silicon and 80 atomic percent palladium was prepared by radio frequency induction melting in a fused silica crucible under an argon atmosphere. The palladium metal, obtained from Engelhardt Industries Inc., was 99.9% pure with an iron content of about 100 parts per million, and the silicon was transistor grade. Small samples of the alloy were rapid-quenched from the molten state by the "piston and anvil" technique [4], producing foils about 3 cm. in diameter and 40 to 50 microns thick. Each foil was examined by means of X-ray diffraction to determine whether any misquench crystals were present. This was done in reflection on a Norelco goniometer using a scanning speed of 0.1°/min. and CuK$_{\alpha}$ radiation. The range of angles covered ($2\theta = 36^{\circ}$ to 44°) included the first broad amorphous band, and any foils that showed either a narrowing of the band or sharp peaks superimposed on the amorphous pattern were rejected (about 60% of those tested). The remaining foils that were large enough to provide a Hall specimen were cut into rectangular strips about 1 cm. wide and four platinum leads were spot-welded along the length of each strip. By means of a potentiometric measurement the temperature coefficient of resistance was determined crudely by comparison of the values at the boiling point of liquid nitrogen and room temperature. The foils showing the

highest residual resistivity, and hence the lowest fractional temperature coefficient of resistance $\frac{1}{R}\frac{dR}{dT}$ were chosen for preparation as Hall effect specimens. In addition, representative foils with lower residual resistivities were also selected. Each of the foils selected for Hall specimen preparation was clamped between two 1/4" thick pieces of brass and milled to the dimensions shown in Figure 1. The "ears" labelled A and B were used to provide the current to the specimens; the Hall voltage was measured between C and D, and the voltage drop between E and F was used to determine the temperature dependence of resistance. A final check for misquench crystals was made on each specimen by taking four or five X-ray exposures in transmission Laue geometry with MoK$_\alpha$ radiation to examine the region between the Hall ears. In none of the exposures was there any indication of granularity to the broad amorphous bands or sharp spots superimposed on them. For the first few specimens, fine platinum wires were spot-welded to each of the ears, but it was found that this method produced an electrically noisy contact probably due to the presence of an A.C. rectifying oxide layer. In later work the contacts were made by soldering fine copper wires to the ears with indium metal.

B. Resistivity and Hall coefficient measurements

The Hall specimen was then connected into the circuit shown in Figure 2. A current of about 200 mA. was provided through the length of the specimen by four parallel 2½ volt railroad batteries
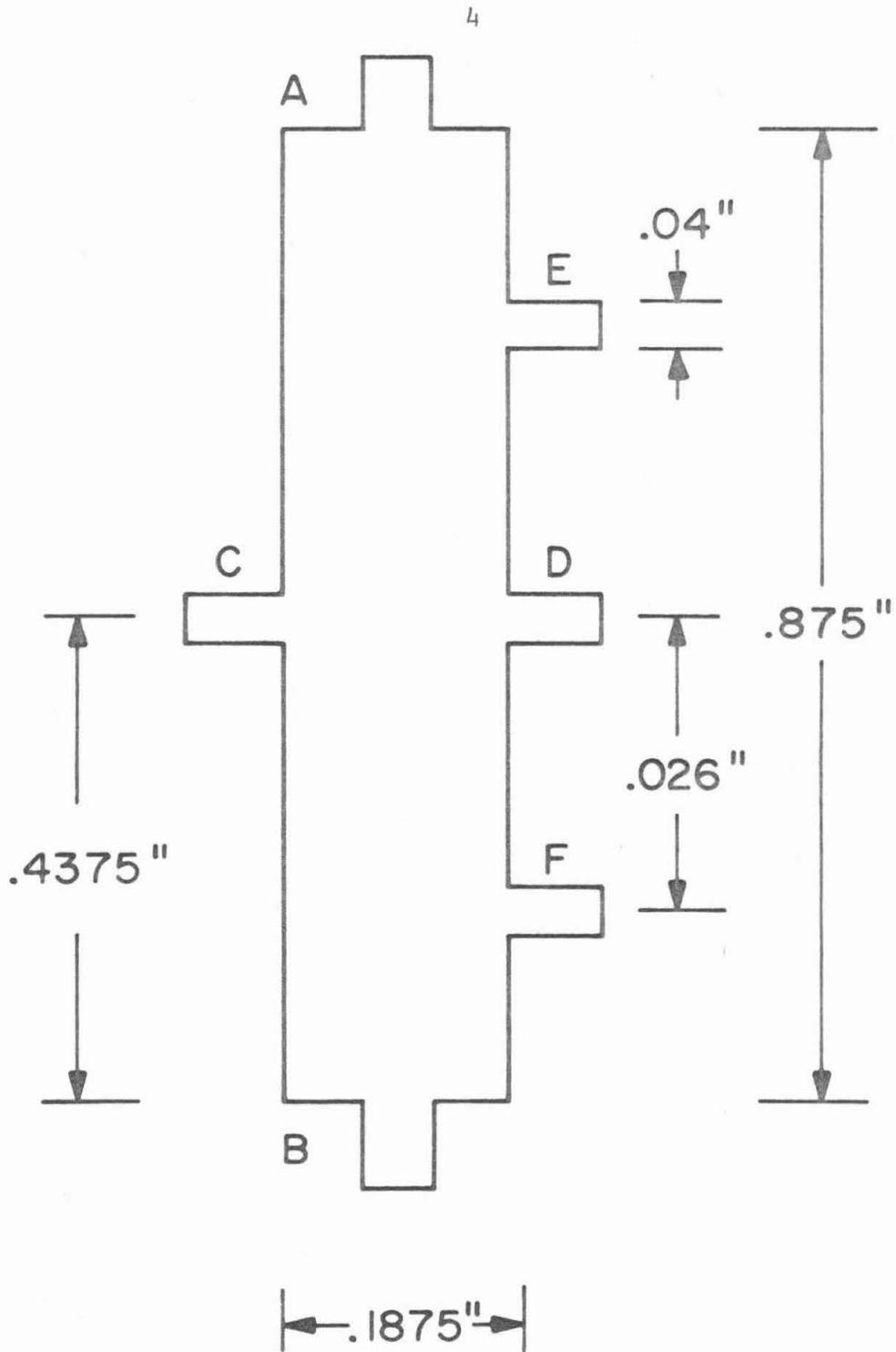
Figure 1. Dimensions of the Hall effect specimens.

("Air cells") in series with a $10\,\Omega$ resistor and a shunt box for measuring the current with a Leeds and Northrup guarded potentiometer. During the measurements this current was stable to one part in 10^6. The guarded potentiometer was also used to measure the voltage drop across the ears E and F in determining the resistance and the voltage developed in a copper-constantan thermocouple circuit with one junction near the specimen and the other in a reference ice bath.

The Hall voltage developed across ears C and D was measured with a Leeds and Northrup Wenner potentiometer. The galvanometer output from the Wenner was fed into a Keithley nanovoltmeter where it was amplified and sent on to an A.Z.A.R. recorder. Most of the voltage (on the order of 10^{-4} volts) across these ears was simply the iR drop due to the fact that the leads could not be located exactly opposite each other. The Hall voltage was much smaller than this (on the order of 10^{-7} volts), so a measurement was performed by reversing the magnetic field and taking half the difference of the voltages for the two field directions as the Hall voltage.

The magnetic field normal to J and E_H was provided by a 12 inch Varian electromagnet with a 2.75 inch pole gap. The magnetic field was measured with a Varian F-8 nuclear magnetic resonance fluxmeter.

In order to reduce noise due to thermoelectric voltages in the Hall circuit and to remove the possibility of a systematic error arising from the Ettinghausen effect, it was found necessary to immerse the specimen in an isothermal bath. For this reason the Hall
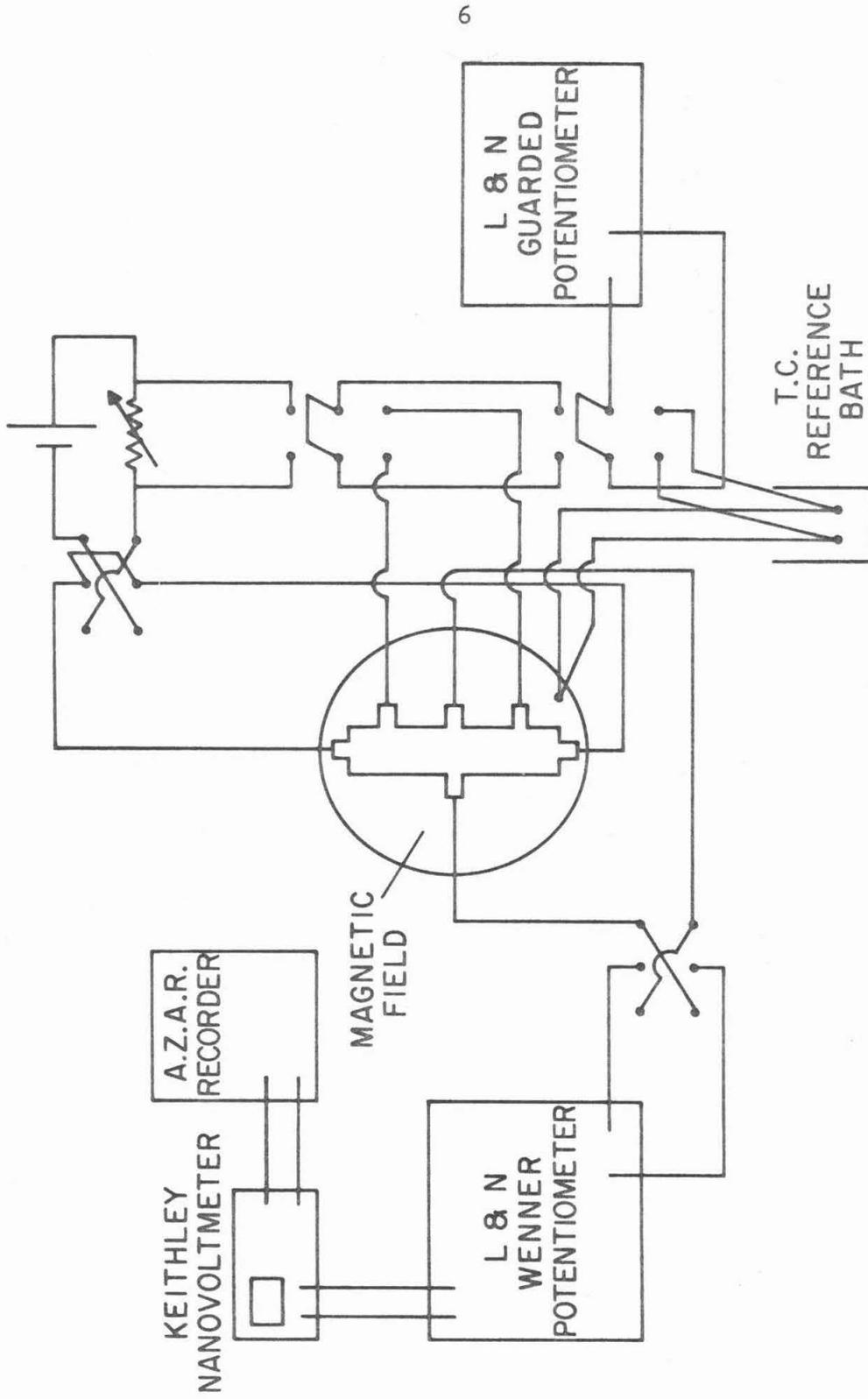
Figure 2. Circuit for measuring Hall coefficient and resistance.

coefficient was measured only at room temperature and the boiling points of liquid He, N_2 and Freon 22. All measurements were made with the specimen in a liquid helium glass Dewar; for the Freon 22 measurements the specimen was immersed in alcohol and the jacket between the liquid He and liquid N_2 containers was filled with He gas to transfer heat to the Freon in the outer Dewar.

At any one temperature the Hall voltage was measured for both directions of current and several values of the magnetic field, in addition to the reversal of field directions already mentioned. The Hall coefficient was found to be independent of field strength and there was no change on reversing the current. The specimens were also tested for transverse magnetoresistance by comparing the potential drop across ears E and F with no magnetic field and with 8 k G. To within the limits of sensitivity of the potentiometer (one part in 10^8) there was no difference.

After the electrical measurements were completed, the thickness of the foils in the region between the Hall ears was determined by taking the average of several readings with a micrometer caliper having a large jaw and a fine one. Attempts to corroborate these measurements with X-ray absorption showed that the foils contained many fine holes. The percent error introduced in the absolute values of the Hall coefficient and resistivity by the thickness measurement was much greater than that due to any other parameter. Fortunately the relative behavior with temperature gives us the most important information about the foils.

C. Additional resistivity measurements

Resistivity values at temperatures between those of the isothermal baths were obtained using the apparatus described in reference (5). The specimens were mounted four at a time inside a brass chamber contained in a liquid helium double dewar. Quasi-isothermal measurements were performed at an interval of about 3°K as the temperature of the chamber gradually rose. About 8 hours were allowed for the range from 4.2^{O}K to 77°K, and the warming from 77°K to room temperature took about 30 hours with an intermittent flow of He gas regulating the rate of temperature rise.

D. Preparation of annealed and equilibrium specimens

In addition to the as-quenched specimens described in part A, a specimen showing no initial crysallinity was sealed under vacuum in a fused silica tube and annealed for 12,000 hours at 225°C. The foil was then re-examined by X-ray diffraction and found to have a small, sharp peak superimposed on the first broad amorphous band.

Another specimen was annealed to the equilibrium phases (Pd_3Si, perhaps Pd_9Si_2 and others) by maintaining it under vacuum at 750°C for one week. Both foils were prepared as Hall specimens and subjected to the measurements described in part B. Because of its brittleness the equilibrium specimen was not mechanically machined to give the correct Hall geometry, but instead electrical discharge machining was used.

III. EXPERIMENTAL RESULTS

The resistance of each specimen, expressed as a ratio to its
room temperature value, is plotted as a function of temperature in
Figure 3. The individual data points have not been reproduced because
they are too closely spaced. The possible error involved in each
measurement is about $\pm$ 0.5°K and $\pm$ 0.1% relative resistance. The
values obtained from the isothermal measurements agreed with these
curves to within the specified accuracy. Specimen No. 140 was
broken before it could be subjected to the quasi-isothermal measure-
ments; its resistivity ratio at liquid He$_2$ temperature was 0.969.
At the same temperature the resistivity ratio for the 12,000-hour
anneal specimen was 0.951 and that for the equilibrium specimen was
0.172.

The negative absolute Hall coefficient of each specimen is
plotted as a function of temperature in Figure 4. The statistical
scatter in repeated measurements of a single data point corresponded
to about $\pm$ 0.1 x 10^{-11}m^3/coulomb, or about $\pm$ 2% of the largest
values obtained, but there is likely to be a much greater error in
the determination of the thickness of each specimen, which enters
as a multiplicative factor for each curve. The size of that error
might be as much as $\pm$ 10%, with the error much more likely to be on
the high side, causing the measured Hall coefficient to be in error
on the high side also, because of the apparent "holes" already
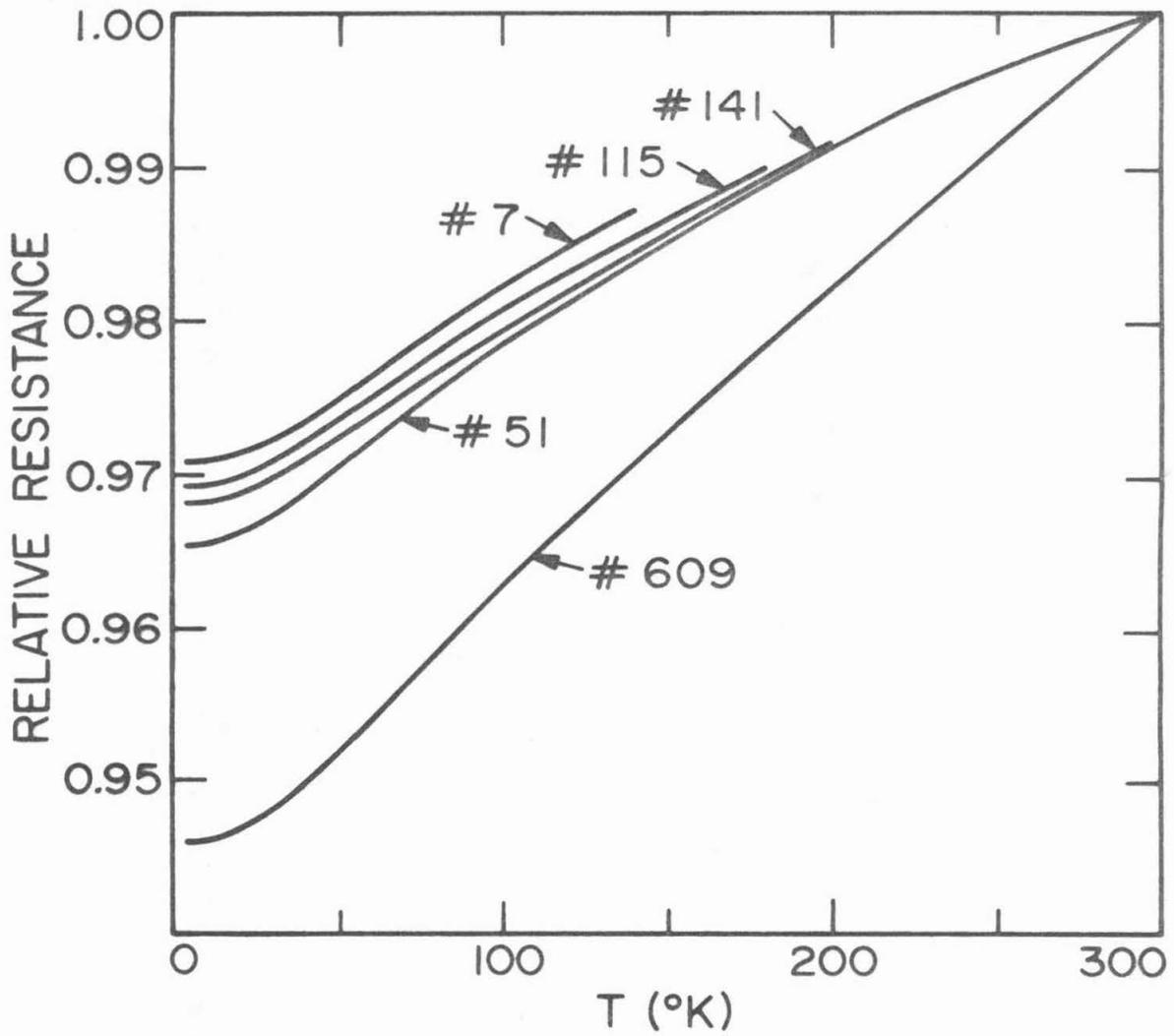
Figure 3. Relative resistance of the specimens versus temperature.
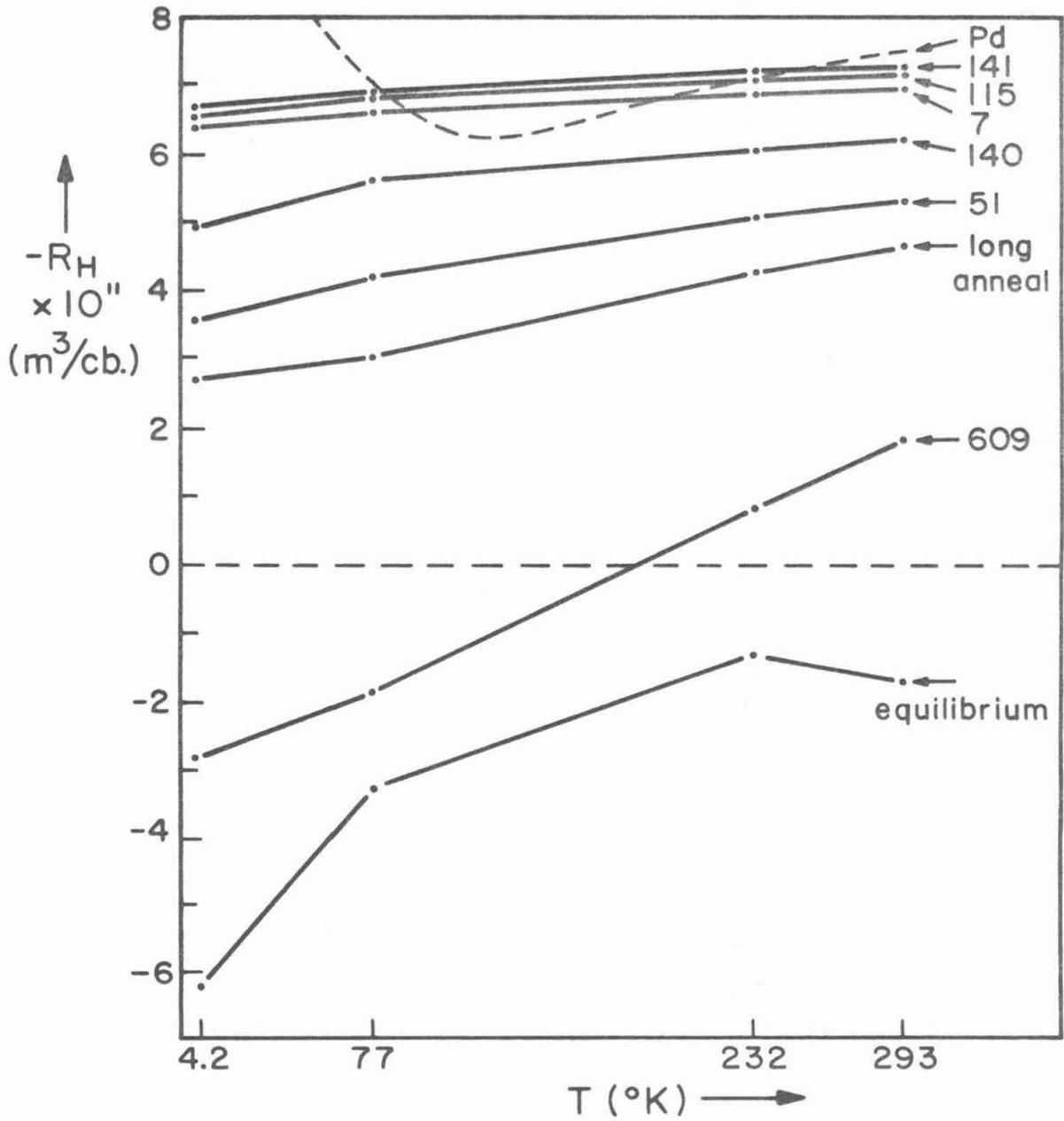
Figure 4. Minus the Hall coefficient as a function of temperature.

mentioned. For this reason we should not attach too much significance to the relative positions of the curves that are fairly close to each other, but we can assume greater reliability for the relative values in any one curve. For purposes of comparison the Hall coefficient of pure palladium obtained by other investigators [6] has also been included.

It will be seen that there does tend to be some correlation in the behavior of these two transport properties from specimen to specimen; the higher the residual resistance at liquid helium temperature the more nearly constant is the Hall coefficient versus temperature curve. (It should be emphasized that Figure 3 is plotted against a greatly expanded portion of the relative resistance scale whereas the ordinate range in Figure 4 includes the value zero, so the Hall coefficient is a much more sensitive indicator of whatever is different in the specimens). Specimen No. 140 is the most noticeable exception to this pattern, having isothermal resistivity ratios that fall consistently between those of specimens 115 and 141, and yet showing considerable curvature in the Hall coefficient plot as well as low values.

Specimen No. 609 was chosen specifically for its relatively low residual resistance after the trend had already been noticed in order to see whether the Hall coefficient could be made to swing positive at low temperatures, as was in fact the case. Strangely enough specimen No. 609 had passed the X-ray test as well as any of

the previous as-quenched specimens and certainly did not show the small, sharp intensity peak that was observed in the 12,000-hour anneal specimen.

The possible error in the relative values for a single curve would indicate that the upward curvature at low temperatures in the long anneal plot is a real feature, and for that reason perhaps this curve should not be classed with the others. The fact that pure palladium shows a strong curvature in the same direction at these temperatures would seem to be consistent with the observation that the position of the first X-ray diffraction peak to appear on annealing is at the exact Bragg angle for the (1, 1, 1) set of planes in pure Pd.[7]

The equilibrium sample, whose X-ray diffraction pattern indicated the presence of Pd_3Si and other unidentified phases (perhaps Pd_9Si_2[8] one of them), is seen to have a consistently positive Hall coefficient. Since this is not a single phase specimen the measured Hall coefficient is some kind of average value, so it is quite possible that one of the phases present might have a much more positive Hall coefficient with either more or less curvature in the temperature dependence.

IV. DISCUSSION

First we shall consider the limiting behavior of these sets of curves as the ideal properties of a "perfect" quench. We would expect a resistivity ratio $R_{4.2^\circ K}/R_{300^\circ K}$ not much greater than 0.97 and a Hall coefficient that is fairly constant with temperature at about $-7 \times 10^{-11} m^3$/coulomb. This value for the Hall constant is typical of a good metal, as is the absolute resistivity of about $80 \times 10^{-6} \Omega$ - cm., and the behavior is what would be expected for a single band model with a spherical Fermi surface. Assuming that model we find that this value corresponds to a density of electrons $n = 1/e R_H$ of around 9×10^{22} per cm^3., and using the previously determined density of about 10 g/cm^3 (3) this is equivalent to 1.7 electrons per palladium atom.

An interesting consequence of this density is that the diameter of the Fermi surface $2 k_f = 2.8 \overset{\circ}{A}^{-1}$ falls right on the first strong peak in the interference function determined from X-ray diffraction data[3]. According to Ziman's pseudopotential theory of liquid metal resistivity this condition would lead to a negative temperature coefficient of resistance, because the strength of that peak is a measure of the electron scattering and it decreases with increasing temperature. The fact that this behavior is not observed in the case of the present solid alloy, whereas it is quite marked in several liquid alloys[9], would seem to be consistent with the

idea that the structural changes with temperature in the liquid state that are responsible for the lowering of the peak in the interference function simply cannot occur in the frozen configuration of the amorphous solid.

A final check on the reasonableness of the Hall coefficient and resistivity results can be made by calculating the mean free path in the free electron model. If we assume that the effective mass is not very different from the true electron mass, an assumption that seems quite valid for many liquid metals[9], then the mean free path is about 9Å, which is physically quite reasonable.

If we now turn our attention to the considerable variation in the temperature dependence of the Hall coefficient from specimen to specimen, we see that the descriptions of this behavior in terms of a single band model is quite impossible, especially in the light of the change of sign for specimen 609. On the other hand, if we assume that the Hall coefficient is properly represented by a two-band formula

$$R_H = \frac{\sigma_1^2 R_{H,1} + \sigma_2^2 R_{H,2}}{(\sigma_1 + \sigma_2)^2}$$

in which $R_{H,1}$ and $R_{H,2}$ are the Hall coefficients for each carrier acting alone and σ_1 and σ_2 are their partial conductivities, and we also assume that R_H is in some way responding to a general change in the whole structure, then we are hard pressed to understand how

R_H could be so much more sensitive to such changes than the conductivity $\sigma = \sigma_1 + \sigma_2$ and the X-ray diffraction tests.

A clue to a possible answer can be found in noticing that while the resistivity of the amorphous material stays quite high at low temperatures, that of the equilibrium crystalline phases falls linearly to a low residual value. Then if there are isolated crystalline regions present with a positive and fairly constant Hall coefficient, the variation of conductivity ratios with temperature could be responsible for the curvature of R_H toward positive values with decreasing temperature. The very first calculation in the next section would seem to discourage this notion, since it shows that for geometrical reasons the current density in an isolated sphere can become no greater than three times that in the surrounding medium, even if the material in the sphere has zero resistivity. But that barely noticeable factor of three becomes more important when it enters as its square in weighting the effect that the Hall coefficient of the crystalline material can have on the whole medium. Finally, the geometrical factor becomes crucial when it is found that it can be made arbitrarily large by varying the shape of the crystalline inclusions in a manner quite consistent with the mechanical aspects of the quenching process.

It now appears that a very small volume fraction of the material in the form of flat, disk-like crystalline regions oriented

parallel to the surface of the specimen could easily account for the observed behavior. Inclusions of this shape would be expected to result from the squashing of initially spherical undissolved crystals or inhomogeneous regions in the melt as the plates of the smasher come together and similarly alter the geometry of the whole specimen. Then in the subsequent examination of the specimens the intensity of diffracted X-rays is sensitive only to the volume fraction of crystalline material, the resistivity is sensitive to that volume fraction weighted by a large geometrical factor and the Hall coefficient is sensitive to the volume fraction weighted by the square of that geometrical factor. The anomalous behavior of specimen 140 can then be explained by invoking a somewhat greater geometrical factor (greater squashing) than is typical of the other specimens.

V.   HALL COEFFICIENT IN A TWO-PHASE SYSTEM

Let us now consider the Hall voltage to be observed for a
system in which a few relatively isolated crystals are present in
an amorphous matrix. This will certainly be relevant to the problem
of misquench crystals (about 1 micron across and well separated) and
should give a qualitative picture of the microcrystalline model.

In many ways this derivation will parallel that of the two-
band model, but the specific topology assumed here (islands of one
phase completely surrounded by the other phase) will lead to
qualitatively different results. As is the case for the two-band
model, we must first determine the current density in each phase
before the magnetic field is applied.

A.   Current density in an isolated crystal

To simplify calculations we will assume that the crystal of
phase 1 (with conductivity σ_1) is a perfect sphere of radius r_o
embedded in phase 2 (with conductivity σ_2) of infinite extent.
This is no great distortion of the real situation because the
observed misquench crystals are nearly round and their diameters are
typically 1/50 the smallest dimension of the specimen. Also the
boundary condition for current flow, that the normal component of
current density vanish at the boundary with an insulator, means that
an exact calculation for a conductor of small rectangular cross
section can be made by placing infinitely many images beside it.

The basic equations governing the current distribution in

a medium of varying conductivity are: [10]

$$\bar{E} = -\nabla V$$

$$\bar{J} = \sigma \bar{E} \quad (\text{Ohm's law})$$

$$\nabla \cdot \bar{J} = 0 \quad (\text{no sources or sinks of } \bar{J}).$$

It will be seen that there is a direct analogy between these equations and those of electrostatics in charge-free space:

$$\bar{E} = -\nabla V$$

$$\bar{D} = \epsilon \bar{E}$$

$$\nabla \cdot \bar{D} = 0 \quad (\text{Gauss's law with no charge}).$$

In the situation under study here, in which σ has just two distinct values in two distinct regions, the first set of equations reduces to

$$\nabla^2 V = 0 \quad (\text{Laplace's equation})$$

in each medium, subject to the boundary conditions $V_1 = V_2$ at the interface (tangential component of $\bar{E}$ is continuous) and $\sigma_1 \nabla_n V_1 = \sigma_2 \nabla_n V_2$ at the interface (normal component of J is continuous).

The coordinate system chosen for this geometry is shown in Figure 5 (top). It will be seen from the symmetry of the problem that the solution should depend only on the distance r from the center of the sphere and the angle θ with respect to the applied field E_0, but not on the azimuthal angle ϕ, the remaining spherical coordinate. In this coordinate system the above
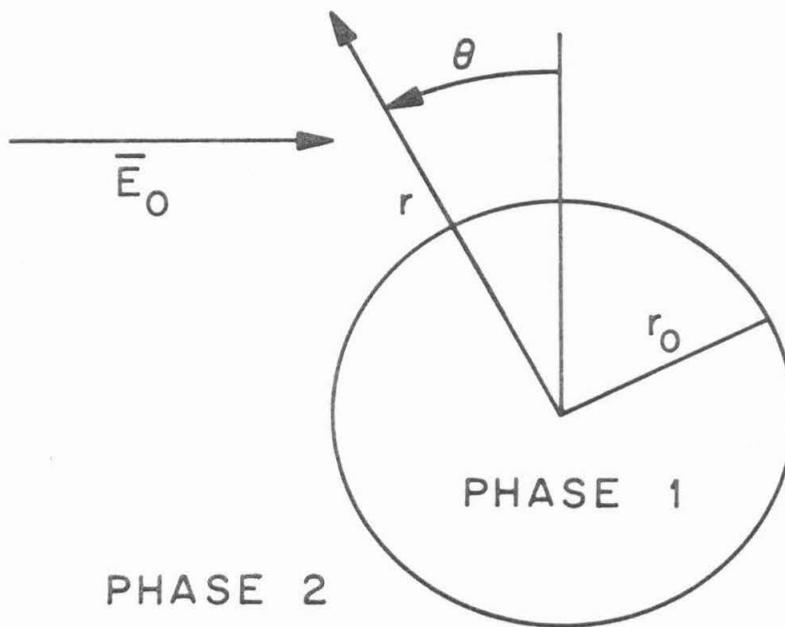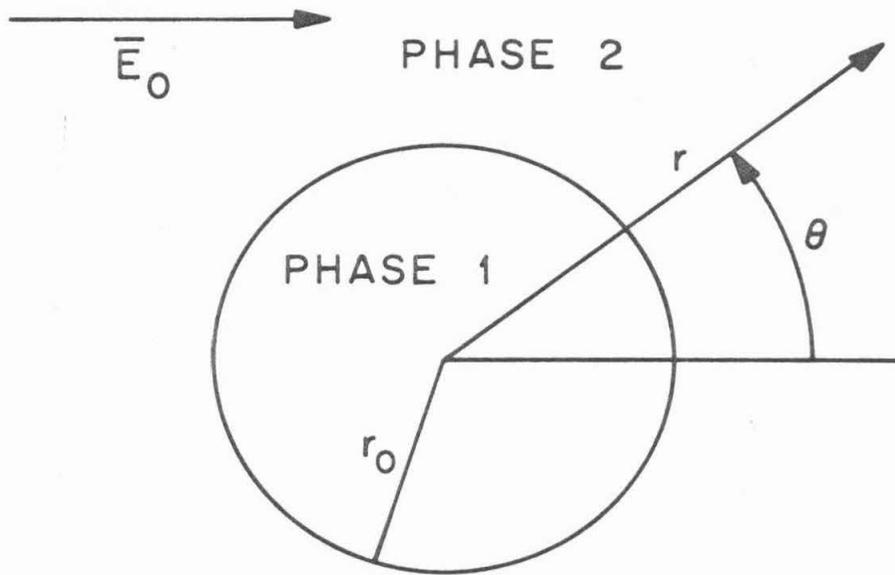
Figure 5. Coordinates for calculation of current density and Hall field in an isolated crystal.

boundary conditions become

$$V_1|_{r_0} = V_2|_{r_0} \quad \text{for all } \theta \tag{1}$$

and

$$\sigma_1 \frac{\partial V_1}{\partial r}\Big|_{r_0} = \sigma_2 \frac{\partial V_2}{\partial r}\Big|_{r_0} \quad \text{for all } \theta. \tag{2}$$

We also have the additional boundary conditions that V_1 is finite

at r = 0 (in order to have $\nabla^2 V|_{r=0} = 0$ $\tag{3}$

and

$V_2 \to -E_0 r \cos \theta$ as $r \to \infty$ (the effects of the sphere must die

off at large distances). $\tag{4}$

Making use of the direct analogy with the equations of

electrostatics we find that the solutions of Laplace's equation in

spherical coordinates are of the form

$$V = \sum_{\ell=0}^{\infty} \sum_{m=0}^{\ell} [A_\ell r^\ell + B_\ell r^{-\ell-1}][C_{\ell,m} P_\ell^m(\cos \theta)$$

$$+ D_{\ell,m} Q_\ell^m(\cos \theta)][E_m \cos m\phi + F_m \sin m\phi]$$

where the P_ℓ^m (x) are the associated Legendre functions. Because

of the symmetry with respect to ϕ already pointed out we must

have $E_m = F_m = 0$ for all values of m ≠ 0, and because all the

$Q_\ell^m (\cos \theta)$ have logarithmic singularities at $\theta = 0, \pi$, we

must have all $D_{\ell,m} = 0$. This leaves

$$V = \sum_{\ell=0}^{\infty} [A_\ell r^\ell + B_\ell r^{-\ell-1}] P_\ell (\cos \theta)$$

where the $P_\ell (x)$ are the Legendre polynomials.

Now if we apply boundary conditions (3) and (4) we see that V_1 must contain no negative powers of r if it is to remain finite at r = 0, and V_2 must include $-E_o$ r $\cos \theta$ but no higher powers of r if it is to have the proper limit as r $\longrightarrow \infty$. Thus if we expand V_1 and V_2 explicitly in terms of the first few Legendre polynomials we obtain

$$V_1 = A_{0,1} + A_{1,1} r \cos \theta + A_{2,1} r^2 (3 \cos^2 \theta - 1) + \cdots$$

and

$$V_2 = (A_{0,2} + \frac{B_{0,2}}{r}) + (A_{1,2} r + \frac{B_{1,2}}{r^2}) \cos \theta + \frac{B_{2,2}}{r^3} (3 \cos^2 \theta - 1) + \cdots$$

The term $\frac{B_{0,2}}{r}$ in V_2 represents a current source or sink, but the sphere is neither so $B_{0,2} = 0$. Now in order to satisfy boundary condition (1) it is clear that if we are to terminate the series, the coefficients of each $P_\ell (\cos \theta)$ in the two series must match at r = r_o. Therefore

$$A_{0,1} = A_{0,2} \text{ (arbitrary constant, doesn't affect}$$
$$\text{the current density)}$$

$$A_{1,1}\, r_o = A_{1,2}\, r_o + \frac{B_{1,2}}{r_o^2} \tag{5}$$

and in general

$$A_{n,1}\, r_o^n = \frac{B_{n,2}}{r_o^{n+1}} \quad \text{for} \quad n \geq 2. \tag{6}$$

Finally, to satisfy boundary condition (2) we must have

$$\sigma_1 \frac{\partial V_1}{\partial r}\Big|_{r_o} = \sigma_1 \left[A_{1,1}\cos\theta + 2 A_{2,1}\, r_o\, (3\cos^2\theta - 1) + \cdots \right]$$

$$= \sigma_2 \frac{\partial V_2}{\partial r}\Big|_{r_o} = \sigma_2 \left[\left(A_{1,2} - \frac{2 B_{1,2}}{r_o^3}\right)\cos\theta - \frac{3 B_{2,2}}{r_o^4}(3\cos^2\theta - 1) + \cdots \right].$$

For the same reason as above we try to match the coefficients of
each $P_\ell(\cos\Theta)$ at $r = r_o$.

$$\sigma_1 A_{1,1} = \sigma_2 \left(A_{1,2} - \frac{2 B_{1,2}}{r_o^3}\right) \tag{7}$$

and in general

$$n\sigma_1 A_{n,1}\, r_o^{n-1} = -(n+1)\,\sigma_2 \frac{B_{n,2}}{r_o^{n+2}} \quad \text{for} \quad n \geq 2. \tag{8}$$

From the boundary condition (4) we must have

$$A_{1,2} = -E_o.$$

Substituting this in (5) and (7) yields

$$A_{1,1} = -E_o + \frac{B_{1,2}}{r_o^3} \quad \text{and} \quad A_{1,1} = \frac{\sigma_2}{\sigma_1}\left(-E_o + \frac{2 B_{1,2}}{r_o^3}\right).$$

Combining these

$$\frac{B_{1,2}}{r_o^3}\left(1+\frac{2\sigma_2}{\sigma_1}\right) = E_o\left(1-\frac{\sigma_2}{\sigma_1}\right)$$

so

$$B_{1,2} = \frac{E_o\, r_o^3\,(\sigma_1-\sigma_2)}{(\sigma_1+2\sigma_2)}$$

and

$$A_{1,1} = A_{1,2} + \frac{B_{1,2}}{r_o^3} = -E_o + \frac{E_o\,(\sigma_1-\sigma_2)}{(\sigma_1+2\sigma_2)}$$

so

$$A_{1,1} = \frac{-3E_o\,\sigma_2}{(\sigma_1+2\sigma_2)}\ .$$

Clearly (6) and (8) can only be satisfied by setting $A_{n,1} = B_{n,1} = 0$ for all $n \geq 2$.

Now let us look at the physical significance of these results. The potential V_1 inside the sphere is simply that of a constant E - field, call it E_1, and there is a corresponding constant current density J_1.

$$E_1 = \frac{3E_o\,\sigma_2}{(\sigma_1+2\sigma_2)} \quad \text{or} \quad \frac{E_1}{E_o} = \frac{3}{\left(2+\frac{\sigma_1}{\sigma_2}\right)}$$

and

$$J_1 = \sigma_1 E_1 = \frac{3E_o\,\sigma_1\sigma_2}{(\sigma_1+2\sigma_2)} = \frac{3J_o\,\sigma_1}{(\sigma_1+2\sigma_2)}$$

so $\quad \dfrac{J_1}{J_0} = \dfrac{3}{(1 + 2\frac{\sigma_2}{\sigma_1})}$.

Notice that E_1/E_0 is hyperbolic when plotted against σ_1/σ_2 and J_1/J_0 is hyperbolic when plotted against σ_2/σ_1. These curves are shown in Figure (6), which is actually two separate graphs, the left-hand one plotted against σ_1/σ_2 for $\sigma_1/\sigma_2 \leqslant 1$ and the right-hand one plotted against σ_2/σ_1 for $\sigma_1/\sigma_2 \geqslant 1$.

The interesting result here is in the two limits $\sigma_1/\sigma_2 \rightarrow 0$ and $\sigma_1/\sigma_2 \rightarrow \infty$. For the case of a poorly conducting sphere we see that E_1 can get no larger than $\frac{3}{2}E_0$. This is quite reasonable because the current flux can easily avoid the small, high-resistance obstacle but still send enough current through it to maintain the boundary condition that the tangential component of $\overline{E}$ be continuous. On the other hand, in the case of a highly conducting sphere one might intuitively expect that J_1/J_0 could go much higher than 3. But we must take into account the other boundary condition -- that the normal component of $\overline{J}$ be continuous at the interface -- which means that to get J_1 much larger than J_0 we would need high current densities in medium 2 near the interface at $\theta \approx 0, \pi$, leading to a large dissipation of energy which defeats the purpose of putting a lot of current through the sphere in the first place. Hence the upper limit on J_1/J_0.
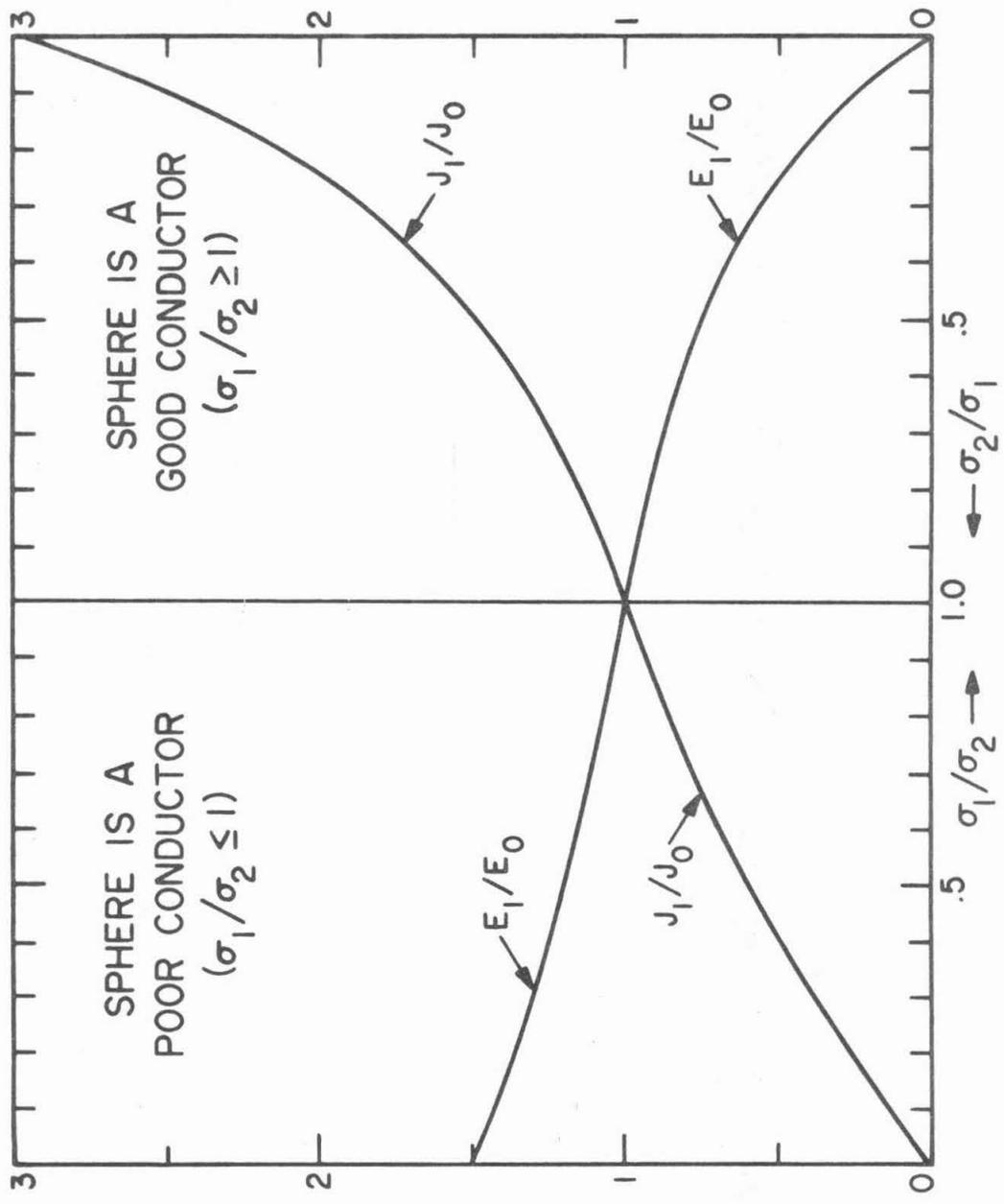
Figure 6. Relative electric field and current density inside an isolated crystal.

B. Effects of many crystals

Now let us determine the effect of a uniform distribution of such spheres on the average resistivity of the whole specimen. If we neglect any detailed interaction between the dipoles then the primary effect is simply the substitution of a certain volume fraction of material, call it v_1, with conductivity σ_1 instead of σ_2, current density $J_1 = 3\sigma_1 J_2 / (\sigma_1 + 2\sigma_2)$ instead of J_2 and electric field $E_1 = 3\sigma_2 E_2 / (\sigma_1 + 2\sigma_2)$ of E_2. The effective conductivity $\langle \sigma \rangle$ of the whole medium is just $\langle J \rangle / \langle E \rangle$ where $\langle \ \rangle$ represents a volume average of either J or E, since these are in fact the quantities that would be detected in measurements of the total current and total potential drop for a macroscopic sample. (It is interesting to note that

$$\langle J / E \rangle = \sigma_1 V_1 + \sigma_2 (1 - V_1)$$

has the effect of putting the two materials in parallel and

$$1 / \langle E / J \rangle = \sigma_1 \sigma_2 / [V_1 \sigma_2 + (1 - V_1)\sigma_1]$$

effectively puts them in series. The correct average falls between the other two expressions, as logically it must, and there are actually much narrower bands that can be put on $\langle \sigma \rangle$ than these two expressions.[11])

In terms of $\sigma_1, \sigma_2, E_1, E_0, V_1$ and $V_2 = (1 - V_1)$ we now have

$$\langle \sigma \rangle = \frac{\langle J \rangle}{\langle E \rangle} = \frac{\sigma_1 V_1 E_1 + \sigma_2 V_2 E_0}{V_1 E_1 + V_2 E_0}$$

$$= \frac{\sigma_1 V_1 \left(\frac{3\sigma_2}{\sigma_1 + 2\sigma_2}\right) E_0 + \sigma_2 (1-V_1) E_0}{V_1 \left(\frac{3\sigma_2}{\sigma_1 + 2\sigma_2}\right) E_0 + (1-V_1) E_0}$$

$$= \sigma_2 \frac{\left[1 + 2V_1 \left(\frac{\sigma_1 - \sigma_2}{\sigma_1 + 2\sigma_2}\right)\right]}{\left[1 - V_1 \left(\frac{\sigma_1 - \sigma_2}{\sigma_1 + 2\sigma_2}\right)\right]} \quad . \tag{9}$$

This relationship is presented in Figure (7) in the form of $\langle\sigma\rangle/\sigma_2$ as a function of v_1 for a few different values of σ_1/σ_2.

Equation (9) should certainly be good in the case where $V_1 \ll 1$ and it is very encouraging that even in the case where v_1 is 1 the expression is reasonable; it becomes exactly equal to σ_1, which is obviously physically right. For the case in which v_1 is $\ll 1$ this expression can be approximated;

$$\langle\sigma\rangle \simeq \sigma_2 \left[1 + 3V_1 \left(\frac{\sigma_1 - \sigma_2}{\sigma_1 + 2\sigma_2}\right)\right]$$

and in the limits;

$$\sigma_1/\sigma_2 \gg 1, \qquad \langle\sigma\rangle \simeq \sigma_2 [1 + 3V_1]$$

and

$$\sigma_1/\sigma_2 \ll 1, \qquad \langle\sigma\rangle \simeq \sigma_2 \left[1 - \frac{3}{2}V_1\right].$$

This is an interesting result in that in either limit the conductivities
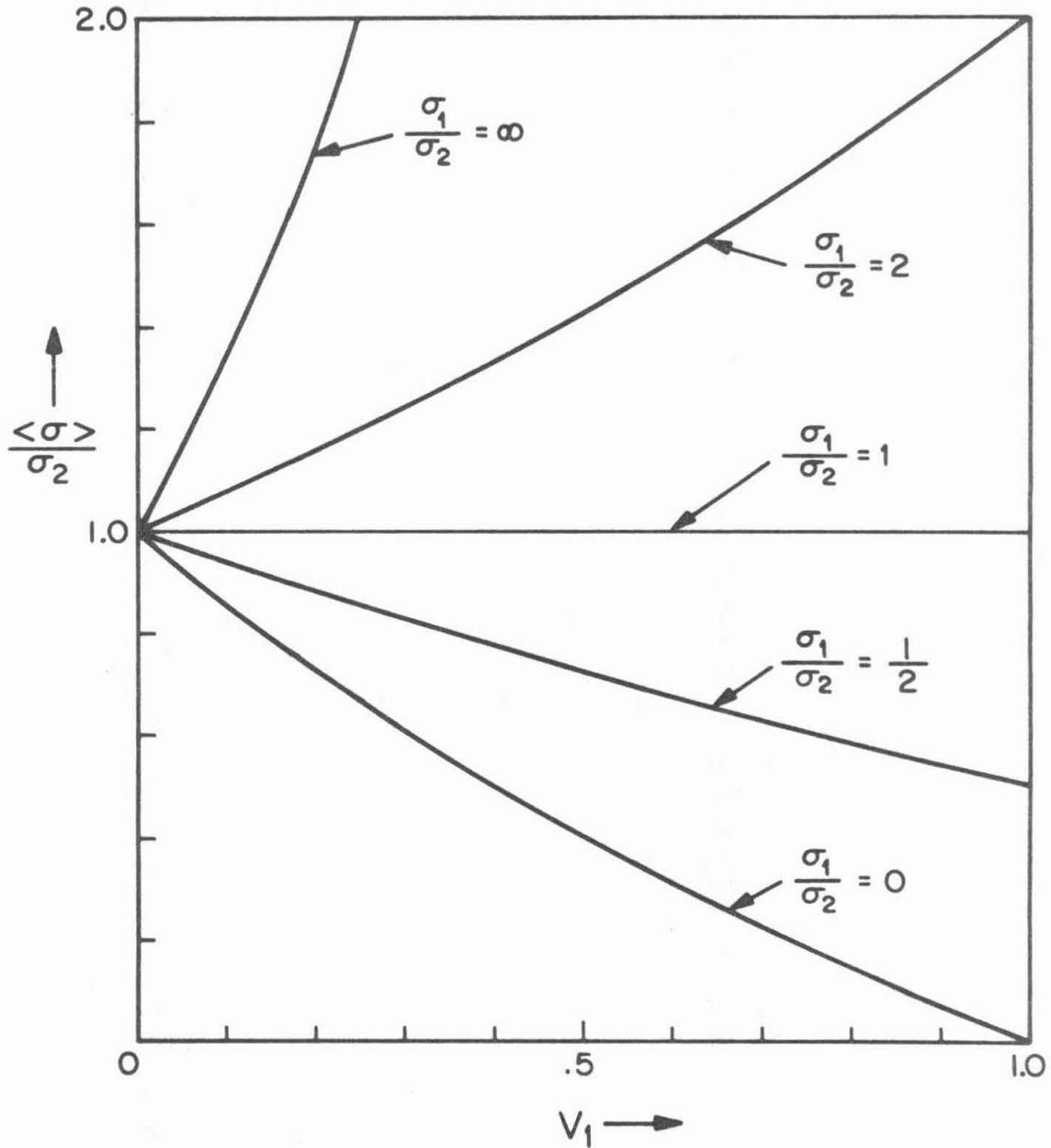
Figure 7. Effective conductivity of the composite medium versus volume fraction of the isolated phase.

or their ratio do not enter into the coefficient multiplying σ_2 so that if we have reason to believe that either limit holds, we can get a good estimate of the volume fraction of phase 1 in different specimens.

If we now attempt to take into account the detailed interactions of the dipoles with a derivation analogous to that for the Claussius-Mossotti equation in the study of dielectric media[12], we will find that equation (9) is already self-consistent as far as depolarization effects are concerned as long as we can treat the spheres as point dipoles and assume a cubic or otherwise isotropic environment about any single dipole. The easiest way to show this is to calculate the depolarization field that arises in the compound medium and show that it is the same as that which appears in the Clausious-Mossotti treatment. Suppose that all the spheres are confined within a specific length of a conductor of uniform cross-section. The requirement of current continuity at the limits of the region containing the spheres then implies

$$\sigma_2 E_{ext.} = \langle J \rangle = \langle \sigma \rangle \langle E \rangle$$

$$= \langle \sigma \rangle (V_1 E_1 + V_2 E_2)$$

$$= \sigma_2 \left(2 V_1 \left(\frac{\sigma_1 - \sigma_2}{\sigma_1 + 2\sigma_2} \right) + 1 \right) E_0$$

from equation (9). Solving for E_o we find

$$E_o = E_{ext.} - 2v_1 \left(\frac{\sigma_1 - \sigma_2}{\sigma_1 + 2\sigma_2}\right) E_o$$

$$= E_{ext.} - 2v_1 \frac{B_{1,2}}{r_o^3} = E_o - \frac{2}{3}(4\pi N_1 B_{1,2})$$

where $N_1 = 3v_1/4\pi r_o^3$ is the number of dipoles per unit volume. But this depolarization field, $-\frac{2}{3}(4\pi N_1 B_{1,2})$, is just the value that would be found at the center of a spherical hole in a slab of material with uniform polarization $4\pi N_1 B_{1,2}$, which is the correct value. (12)

After performing this calculation I have found that it was done originally by none other than Maxwell himself (13). As might be expected, the calculation has reappeared at various times in the literature relating to electrical resistance, dielectric behavior, thermal conductivity and magnetic behavior (all of them fields governed by analogous equations leading to essentially the same boundary value problem) incorporating real or imagined improvements on the Maxwell result (14).

A justly famous example is Lord Rayleigh's calculation that takes into account the detailed interaction of the dipole moments in a particular arrangement (simple cubic array of spheres) (15). The correction to the Maxwell formula, which is an octupole term arising from the finite size of the spheres, is negligible over the volume fraction range that Rayleigh considered $(0 \leq V_1 \leq 0.4)$ for even the extreme limits of σ_1/σ_2, but the importance of this paper lies in its introduction of Green's function techniques in what is

essentially a solid state problem. Two well-known later applications

of these techniques are Ewald's dynamical theory of X-ray dif-

fraction[16] and the Kohn-Korringa-Rostoker energy band calculation[17].

An interesting modification of Maxwell's calculation that

attempts to treat a statistical mixture with large v_1 and similar

particle size for the two components is that of D.A.G. Bruggeman[18].

According to this treatment a differential volume fraction of phase 1

is introduced into a uniform medium whose conductivity is the same as

the effective conductivity of the true two-phase system. A differen-

tial change in effective conductivity of the system is then calculated

by the Maxwell formula, and these differential changes are integrated

to find the relationship between $\langle\sigma\rangle$ and v_1;

$$\frac{\langle\sigma\rangle - \sigma_1}{\sigma_2 - \sigma_1} = \left(\frac{\langle\sigma\rangle}{\sigma_2}\right)^{1/3}(1 - V_1).$$

Numerical values of $\langle\sigma\rangle$ for specific volume fractions can

be obtained by successive approximations starting with the Maxwell

result. The deviation from the Maxwell result for this calculation

is in the same direction as for Rayleigh's calculation -- the effect

of the crystals on $\langle\sigma\rangle$ is greater for both signs of $(\sigma_1 - \sigma_2)$ --

but the magnitude is considerably greater. For $v_1 = 0.4$ and

$\sigma_1/\sigma_2 = 0$, Rayleigh's $\langle\sigma\rangle$ differs from Maxwell's by only 0.5%

while Bruggeman's is 7.0% low. For larger v_1 Bruggeman's modification

has increasingly greater effect until at $v_1 = 0.8$ his $\langle\sigma\rangle$ is only

63% of Maxwell's. (Comparison with Rayleigh's result is out of the

question because the geometry he assumed cannot exist with $v_1 > 52\%$ and

his $\langle\sigma\rangle$ has already gone to zero at $v_1 = 0.76$).

Some experimental tests of these and other formulas tend to support the original Maxwell result in cases where one phase is definitely discontinuous and the other is continuous. (The Bruggeman formula is probably better in systems where the two components are equivalent). Determinations of the effective dielectric constant of sintered UO_2 as a function of porosity over the range $0 \leq v_1 \leq 0.4$ ($\epsilon_1/\epsilon_2 \simeq 0.05$) were unable to distinguish between the Maxwell, Rayleigh and Bruggeman formulas, but three other formulas definitely failed to fall within the experimental error bars[19]. A very straightforward test of these formulas has been carried out by arranging macroscopic segments of spherical insulators in a triangular shaped trough of conducting liquid in both simple cubic and hexagonal close packed arrays and simply measuring the total resistance between the ends. To the limits of v_1 (0.75 for h.c.p.) the results showed excellent agreement with Maxwell's formula, and the precision of the measurements was such that the Bruggeman formula clearly failed[20].

C. The Hall voltage

We will now solve for the potential V associated with the transverse voltages that arise when a magnetic field is applied to the specimen at right angles to the direction of the current density J. Let us rotate the coordinate system through $\pi/2$ as shown in Figure 5 (bottom) so that $\theta = 0$ is now in the direction $\vec{J} \times \vec{B}$. ($\vec{B}$ is directed into the paper). Because the symmetry is the same as that for the problem in section (A), the solution will have the same form. Rather than carry through such a formal calculation again we shall simply make use of the previous results.

There is one important difference between the present problem and the previous one; there are now active seats of electromotive force distributed throughout the system. Specifically, the Hall effect acts like a continuous density of batteries with internal resistance depending on the local resistivity, spread out uniformly over any one phase. The problem of the Hall field due to an isolated sphere embedded in a different medium is exactly analogous to the magnetic problem of a uniformly magnetized sphere, with electromotive force playing the same role as magnetomotive force.

If we first consider the case in which the isolated sphere has much greater conductivity than the medium, then we find essentially the full Hall e.m.f. developed across any chord of the sphere in the transverse direction. This corresponds to a battery with its

terminals open-circuited, so the internal resistance has no effect. On the boundary $r = r_o$ we have

$$\mathcal{E}_H = R_{H,1} \, J_1 \, B \, r_o \, \cos \theta$$

where $\mathcal{E}_H$ is the Hall e.m.f. (or voltage) relative to the center of the sphere and J_1 is the uniform longitudinal current density in the sphere. For the single sphere this Hall e.m.f. on the surface gives rise to a dipole field in the surrounding medium with

$$\frac{B_{1,2}}{r_o^3} = R_{H,1} \, J_1 \, B$$ to satisfy boundary condition

(1). ($A_{1,2}$ is zero because there is no uniform external transverse field at this point in the calculation). With a volume fraction v_1 of such dipoles present the depolarization field of magnitude

$-3 \, v_1 \dfrac{B_{1,2}}{r_o^3}$ would be measured experimentally as the Hall field of the

composite medium.

   Now as we gradually reduce σ_1/σ_2 from an arbitrarily large value we begin to draw current from the battery, so the internal resistance starts to have effect. The potential at the boundary is reduced by the potential drop due to transverse current flow inside the sphere and we now find

$$\frac{B_{1,2}}{r_o^3} = R_{H,1} \, J_1 \, B - \frac{J_{H,1}}{\sigma_1} \qquad (10)$$

where $J_{H,1}$ is the transverse current density inside the sphere. To

satisfy boundary condition (2) we must have

$$J_{H,1} = \sigma_2 \frac{2 B_{1,2}}{r_o^3}. \tag{11}$$

Substituting this into equation (10) and solving for the dipole coefficient we obtain

$$\frac{B_{1,2}}{r_o^3} = \frac{R_{H,1} J_1 B}{\left(1 + 2 \frac{\sigma_2}{\sigma_1}\right)}. \tag{12}$$

From this we see that in the other extreme limit, $\sigma_1/\sigma_2 = 0$, the battery is completely shorted out by the surrounding medium and no Hall field develops. As might be expected the total current density in the sphere is then flowing at the Hall angle $= tan^{-1} \sigma_1 R_{H,1} B$ with respect to $\bar{E}_o$. Notice that, except for a factor of three,

$$\frac{B_{1,2}}{r_o^3 (R_{H,1} J_1 B)}$$ has the same functional dependence on σ_1/σ_2

as does J_1/J_o, which is plotted in Figure 6.

     Once again we can take into account some of the interaction among the dipoles by making the dipole coefficient consistent with the depolarization field. Instead of equation (10) we now have

$$\frac{B_{1,2}}{r_o^3} (1 + 2 v_1) = R_{H,1} J_1 B - \frac{J_{H,1}}{\sigma_1}$$

from boundary condition (1), and instead of equation (1), we have

$$J_{H,1} = \sigma_2 \frac{B_{1,2}}{r_o^3} (2 - 2 v_1)$$

from boundary condition (2). Again solving for the dipole coefficient we obtain

$$\frac{B_{1,2}}{r_0^3} = \frac{R_{H,1} J_1 B}{[1 + 2v_1 + \frac{\sigma_2}{\sigma_1}(2 - 2v_1)]}$$

$$= \frac{\sigma_1 R_{H,1} J_1 B}{[\sigma_1 + 2\sigma_2]} \cdot \frac{1}{[1 + 2v_1 \frac{(\sigma_1 - \sigma_2)}{(\sigma_1 + 2\sigma_2)}]}$$

$$= \frac{3\sigma_1^2 R_{H,1} \langle J \rangle B}{[\sigma_1 + 2\sigma_2]^2 [1 + 2v_1 (\frac{\sigma_1 - \sigma_2}{\sigma_1 + 2\sigma_2})]^2} , \qquad (13)$$

and of course the depolarization or Hall field that would be measured is just $-3 v_1$ times this.

For the case $\sigma_1 / \sigma_2 \gg 1$ we can simplify this to an effective Hall coefficient

$$\langle R_H \rangle = \frac{9 v_1 R_{H,1}}{(1 + 2v_1)^2}$$

which shows the geometrical amplification factor of nine in the numerator and the depolarization terms in the denominator. For the case $v_1 \ll 1$ we obtain from equation (13)

$$\langle R_H \rangle = \frac{9 v_1 \sigma_1^2 R_{H,1}}{[\sigma_1 + 2\sigma_2]^2}$$

which shows a marked similarity to the two band formula.

D. The geometrical amplification factor

The problem of the general ellipsoid with arbitrary orientation in a uniform external field involves the depolarization or demagnetizing factors of the ellipsoid.[12] The problem was first solved by Poisson for the magnetic case, and an interesting result of the calculation is the fact that the field inside the ellipsoid is uniform. We shall consider here only the special cases of oblate and prolate spheroids with their axes of revolution aligned perpendicular or parallel to the external field; in these cases the internal field is parallel to the external field, and the depolarization factors are available in analytic (though not very convenient) form.[13]

Because of the complexity of the calculation, no attempt at rigor will be made in this section. Instead, the major equations of the previous sections will be presented with the appropriate general depolarization factor in place of the particular value $4\pi/3$ for the sphere. The equations resulting from this procedure are valid and can be verified by referring to the first appendix of reference (21).

Boundary condition (1) requiring continuity of the potential now implies

$$A_{b,1} = -E_o + B_{1,2}\frac{\eta}{V_o}$$

and boundary condition (2) on the normal component of current density requires

$$\sigma_1 A_{b,1} = \sigma_2 \left(-E_o - B_{1,2}\frac{(4\pi - \eta)}{V_o}\right)$$

where v_o is the volume of the ellipsoid and η its depolarization factor for the given direction of $\bar{E}_o$. In solving these and subsequent equations we will find it convenient to define a new parameter $\alpha = (4\pi/\eta) - 1$. We find that the internal field strength is

$$E_1 = -A_{1,1} = E_o \frac{\sigma_2}{\sigma_1} \frac{(\alpha + 1)}{(1 + \alpha \frac{\sigma_2}{\sigma_1})}$$

and the dipole coefficient in the surrounding medium is

$$B_{1,2} = E_o \frac{v_o}{\eta} \frac{(1 - \sigma_2/\sigma_1)}{(1 + \alpha \sigma_2/\sigma_1)}.$$

The current density ratio is then

$$J_1 / J_2 = \frac{(\alpha + 1)}{(1 + \alpha \frac{\sigma_2}{\sigma_1})}$$

and the effective conductivity becomes

$$\langle \sigma \rangle = \frac{\left[1 - V_1 + \frac{(\alpha + 1) V_1}{(1 + \alpha \sigma_2/\sigma_1)} \right]}{\left[\frac{1 - V_1}{\sigma_2} + \frac{(\alpha + 1)}{(1 + \alpha \sigma_2/\sigma_1)} \frac{V_1}{\sigma_1} \right]}.$$

To get this in a form that will be somewhat comparable to the formula for the effective Hall field we should invert the expression to obtain

$$\langle \rho \rangle = \frac{(1 - V_1) \rho_2 + V_{eff.} \rho_1}{1 - V_1 + V_{eff.}}$$

in which the effective volume $V_{eff} = \frac{(\alpha + 1)}{(1 + \alpha \sigma_2/\sigma_1)} v_1$ is different from v_1 because it includes the effect of the current density ratio.

The equations for the calculation of the Hall coefficient

become modified in a similar manner. Instead of equation (10) we now have

$$\frac{\eta}{V_0} B_{1,2}(1+\alpha V_1) = R_{H,1} J_1 B - \frac{J_{H,1}}{\sigma_1}$$

and instead of equation (11)

$$J_{H,1} = \sigma_2 \frac{\alpha \eta}{V_0} B_{1,2}(1-V_1).$$

Solving these we find

$$B_{1,2} = \frac{V_0}{\eta} \cdot \frac{R_{H,1} J_1 B}{\left(1+\alpha \frac{\sigma_2}{\sigma_1}+\alpha V_1\left(1-\frac{\sigma_2}{\sigma_1}\right)\right)}.$$

At this point we can again identify the depolarization field with the effective Hall-field

$$-4\pi N_1 B_{1,2} = -\frac{4\pi V_1}{\eta} \cdot \frac{R_{H,1} J_1 B}{\left(1+\alpha \frac{\sigma_2}{\sigma_1}+\alpha V_1\left(1-\frac{\sigma_2}{\sigma_1}\right)\right)}$$

where again the volume fraction v_1 is occupied by N_1 ellipsoids per unit volume, each of volume v_0.

Because of the importance of this result, it might be valuable to derive it by the same line of reasoning as is used in the two-band model. A proper measurement of the Hall coefficient requires that the transverse current be zero. Applying this condition yields

$$\langle J_H \rangle = (1-V_1)\sigma_2 E_{H,2} + V_1 J_{H,1} = 0$$

or

$$E_{H,2} = -v_1 \frac{\alpha \eta}{v_0} B_{1,2} \cdot$$

then

$$\langle E_H \rangle = (1-v_1) E_{H,2} + v_1 E_{H,1}$$

$$= -v_1(1-v_1)\frac{\alpha \eta}{v_0} B_{1,2} - v_1 \left(R_{H,1} J_1 B - \frac{J_{H,2}}{\sigma_1} \right)$$

$$= -v_1 \frac{(\alpha+1)\eta}{v_0} B_{1,2} = -4\pi N_1 B_{1,2}.$$

The minus sign in the contribution to $\langle E_H \rangle$ from the volume
fraction v_1 is consistent with the fact that in the Hall batteries
the current is flowing uphill in potential.

We now find the effective Hall coefficient

$$\langle R_H \rangle = \frac{-\langle E_H \rangle}{\langle J \rangle B} = \frac{4\pi v_1 R_{H,1} J_1}{\langle J \rangle \eta_\perp (1 + \alpha_\perp \frac{\sigma_2}{\sigma_1} + \alpha_\perp v_1(1-\frac{\sigma_2}{\sigma_1}))}$$

$$= \frac{(\alpha_\perp +1) v_1 R_{H,1}}{[1 + \alpha_\perp \frac{\sigma_2}{\sigma_1} + \alpha_\perp v_1(1-\frac{\sigma_2}{\sigma_1})]} \frac{J_1}{\langle J \rangle}$$

where the subscript $\perp$ is used to acknowledge the fact that the
depolarization factor in the direction of the Hall field, and hence
perpendicular to current density, may be different from that in the
direction of current flow, call it $\eta_{\parallel}$. Then

$$\frac{J_1}{\langle J \rangle} = \frac{(\alpha_{\parallel} +1)}{[1 + \alpha_{\parallel}\frac{\sigma_2}{\sigma_1} + \alpha_{\parallel} v_1(1-\frac{\sigma_2}{\sigma_1})]}$$

and

$$\langle R_H \rangle = \frac{(\alpha_\perp +1)(\alpha_{\parallel} +1) v_1 R_{H,1}}{[1+\alpha_\perp \frac{\sigma_2}{\sigma_1} + \alpha_\perp v_1(1-\frac{\sigma_2}{\sigma_1})][1+\alpha_{\parallel}\frac{\sigma_2}{\sigma_1} + \alpha_{\parallel} v_1(1-\frac{\sigma_2}{\sigma_1})]}$$

$$= \frac{(\alpha+1)^2 \, V_1 \, R_{H,1}}{\left[1 + \alpha \frac{\sigma_2}{\sigma_1} + \alpha V_1 \left(1 - \frac{\sigma_2}{\sigma_1}\right)\right]^2}$$

in the present case where $\alpha_\perp = \alpha_{\parallel}$. Notice that the
effective volume $v_{eff.}$ that we would define here involves the square
of the factor that appears in the effective volume for resistivity
except for the depolarization term $\alpha V_1 \left(1 - \frac{\sigma_2}{\sigma_1}\right)$ in the denominator.
Notice also that just as in the case of the original Maxwell result
the expressions for both $\langle R_H \rangle$ and $\langle \sigma \rangle$ go to the right limit as
$V_1 \rightarrow 1$.

So far this section has been quite abstract and it might help
to look at the general behavior of η and α and the values of various
expressions in specific cases. Unfortunately the general expression
for η is an elliptic integral and the special forms for symmetrical
cases are still difficult to interpret. Some limiting values can be
obtained from the facts that the sum of the three η's for an
ellipsoid is 4π and that a large η is associated with a small
dimension of the ellipsoid. Thus the range of values for η is 0
to 4π and the corresponding α varies from ∞ to 0 . For the case
of a disk oriented normal to the flow of current $\eta = 4\pi, \alpha = 0,$
$J_1 = J_2$ and $E_1 = \frac{\sigma_2}{\sigma_1} E_0,$ as we know must be the case from the current
continuity requirement. For a rod with its axis perpendicular to the
current $\eta = 2\pi, \alpha = 1, J_1 = \frac{2\sigma_1}{\sigma_1 + \sigma_2} J_2$ and $E_1 = \frac{2\sigma_2}{\sigma_1 + \sigma_2} E_0,$ which can

be verified by the two-dimensional boundary value calculation. For a disk with its thin dimension (call it a , and the other dimension c) oriented normal to the current, $\eta \to \pi^2 \frac{a}{c}$ as $a/c \to 0$ and the effective volume for resistivity $\to \frac{4c}{\pi a} V_1$ for superconducting inclusions. This effective volume is $4/\pi$ times the volume of a sphere with the same diameter as the disk. For a rod with its axis parallel to the current flow $\eta \to 4\pi (a^2/c^2)(\ln \frac{2c}{a} - 1)$ as $a/c \to 0$ where c is the length of the rod and a is its diameter. Because of the logarithmic term the effective volume for resistivity would diverge for superconducting inclusions of finite length, clearly a non-physical result. For finite σ_1 in either of these latter cases $v_{eff.} \to (\sigma_1/\sigma_2) V_1$, which shows that we are just putting the material of the inclusions in parallel with the surrounding material. The series case is represented by the disk normal to the current flow, for which $v_{eff.} = v_1$.

E. The Hall coefficient of the connected phase

If we now allow the Hall coefficient $R_{H,2}$ of phase two to be non-zero, we shall find that there are two major effects of the inclusions on $\langle R_H \rangle$: there is a modification of the longitudinal J_2 by the presence of phase I with different conductivity, and the depolarization field from the dipoles now adds to the normal Hall field - $R_{H,2} J_2 B$. The circulating currents that flow in the specimen because $R_{H,2} J_2$ differs from $R_{H,1} J_1$ are still due to the dipoles that

we have already examined, but these now have a dipole strength

$$B_{1,2} = \frac{(R_{H,1} J_1 - R_{H,2} J_2) B}{[1 + \alpha \, \sigma_2/\sigma_1 + \alpha V_1 (1 - \frac{\sigma_2}{\sigma_1})]}.$$

This line of reasoning quickly yields an effective Hall coefficient

$$\langle R_H \rangle = \frac{R_{H,2} J_2}{\langle J \rangle} + \frac{(\alpha+1) V_1 (R_{H,1} J_1 - R_{H,2} J_2)}{[1 + \alpha \sigma_2/\sigma_1 + \alpha V_1 (1 - \frac{\sigma_2}{\sigma_1})] \langle J \rangle}$$

$$= \frac{R_{H,2} (1-V_1)(\sigma_1 + \alpha \sigma_2)^2 + R_{H,1} V_1 \sigma_1^2 (1+\alpha)^2}{[\sigma_1 + \alpha \sigma_2 + \alpha V_1 (\sigma_1 - \sigma_2)]^2}.$$

The second form again shows a similarity to the two-band model, although the presence of v_1 in the numerator and denominator spoils a perfect analogy. Notice that in the case $R_{H,2} = 0$, the present form reduces to the previous one involving only $R_{H,1}$, and when $R_{H,1} J_1 = R_{H,2} J_2$ we get an effective Hall coefficient that is just $R_{H,2}$ enhanced or diminished by the ratio $J_2/\langle J \rangle$, as we would expect. Another limiting case, in which $\sigma_1 = 0$, yields

$$\langle R_H \rangle = R_{H,2}/(1-V_1)$$

and allows comparison with the only direct calculation for the Hall coefficient that I have found in the literature. For this case Juretschke, Landauer and Swanson[22] obtained an additional factor in the numerator ranging from $(1 - v_1)$ for cylinders perpendicular

to both $\langle \bar{J} \rangle$ and $\langle \bar{E} \rangle$, through $(1 - \frac{1}{4}v_1)$ for spheres and finally to 1 for disks with their axes perpendicular to both $\langle \bar{J} \rangle$ and $\langle \bar{E} \rangle$. The two different results agree for the last geometry, and they are clearly correct because the effect of the disks is simply to do nothing more than introduce an error in the thickness of the specimen. The discrepancy appears to be due to my failure to include the effects of the magnetic field on the dipole currents in phase one.

F. Magnetoresistance

Any time that a Hall electromotive force is shorted out in any way we can expect to observe a transverse magnetoresistance effect. This is shown most simply in the case of the two-band model with carriers of different mobilities, and Conyers Herring has shown in a very important paper[23] that small spacial fluctuations in the Hall coefficient can prevent high field saturation of the magnetoresistance. In both these cases, as with the present one, there can be transverse motion of changes while at the same time there is no net transverse current.

The simplest way to show the effect in the present case is to compare the power dissipation per unit volume with the magnetic field on to that with the field off. With no magnetic field the Joule heating per unit volume is just $P = \langle \rho \rangle \langle J \rangle^2.$

A good approximation with the field on is then

$$P = <\rho><J>^2 + V_1 \frac{J_{H,1}^2}{\sigma_1} + \frac{1-V_1}{\sigma_2}\left(\frac{V_1 J_{H,1}}{1-V_1}\right)^2$$

where the requirement of no net transverse current has been used to evaluate the average current density in phase 2. Strictly speaking there should also be a term representing the interaction of the Hall dipole current with the longitudinal J_2.

The calculation will not be carried out in all its gory details, but just far enough to show the typical B^2 dependence. We have

$$\Delta <\rho> = \frac{\Delta P}{<J>^2} = \left(\frac{V_1}{\sigma_1} + \frac{V_1^2}{(1-V_1)\sigma_2}\right)\frac{J_{H,1}^2}{<J>^2}$$

$$= \frac{1}{<J>^2}\left(\frac{V_1}{\sigma_1} + \frac{V_1^2}{(1-V_1)\sigma_2}\right)\left[\sigma_2 \propto (1-V_1)\frac{(R_{H,1}J_1 - R_{H,2}J_2)B}{[1+\alpha\frac{\sigma_2}{\sigma_1}+\alpha V_1(1-\frac{\sigma_2}{\sigma_1})]}\right]^2.$$

This equation also shows the non-saturation at high fields that we would expect in this case.

G. Application to the present results

We shall now adjust some of the parameters affecting $\langle \rho \rangle$ and $\langle R_H \rangle$ to produce the kind of variations observed experimentally and try to see whether these parameters are consistent with reasonable values for the Hall coefficient and resistivity of the crystalline inclusions. The criterion for such a test will be the predicted value of the Hall mobility $\mu_{H,1} = R_{H,1} \sigma_1$ for the crystalline phase. Because the variations $\Delta \rho$ and ΔR_H of the better-behaved specimens would be quite sensitive to the ideal amorphous values that were chosen, we will concentrate only on specimen No. 609. It seems fairly clear that the other curves in Figure 4 could then be explained by keeping the other parameters fairly constant and just decreasing the true volume fraction v_1.

Unfortunately the minimum mobility required to explain the behavior of specimen 609 is quite sensitive to the v_1 chosen; conceivably a v_1 as large as .01 might go undetected by X-ray diffraction, so we will assume that value for the sake of argument. A good approximation to the fractional change in resistivity is

$$\frac{\Delta \rho}{\rho} \simeq v_{eff}\left(1 - \sigma_2/\sigma_1\right) = \frac{(\alpha+1)\, v_1 \left(1 - \sigma_2/\sigma_1\right)}{\left(1 + \alpha\, \sigma_2/\sigma_1\right)},$$

which should be about .025 for No. 609 at 4.2°K. A reasonable geometry for a disk might be to have its thickness about one tenth its diameter, corresponding to an η of 0.87 and an α of 13.4.

Substitution in the equation above yields

$$\sigma_2/\sigma_1 \simeq 0.25 \quad \text{and} \quad V_{eff} \simeq 3.3 \, V_1.$$

An equally good approximation for the change in the Hall coefficient is

$$\Delta R_H \simeq \frac{(\alpha+1)^2}{(1+\alpha \, \sigma_2/\sigma_1)^2} \, V_1 \, R_{H,1}$$

which is about 0.11 $R_{H,1}$ using the same assumed values. At 4.2°K, ΔR_H is about 10/7 $R_{H,2}$ so we must have $R_{H,1} \simeq 14 \, R_{H,2}$, and combining this with the conductivity ratio we find $\mu_{H,1} \simeq 56 \, \mu_{H,2}$. As an indication of the sensitivity to v_1 of this result, if we change v_1 to .015 then $\mu_{H,1}$ drops to about $40 \, \mu_{H,2}$. Decreasing the thickness to diameter ratio will not cause much change in this range, but if we increase it by a factor of two, keeping $v_1 = .01$, then $\mu_{H,1}$ rises to $70 \, \mu_{H,2}$.

From the mobility of the idealized amorphous material, which is about 0.9 cm^2/v-sec, we see that $\mu_{H,1}$ should be about 50 cm^2/v-sec at liquid helium temperature. Unfortunately there seems to be no information available on the mobility of Pd_3 Si or any other compound in this system. The most nearly comparable phase for which a value is readily available is Pt Si, with a room temperature mobility of 13 cm^2/v-sec compared to 0.8 cm^2/v-sec for pure platinum[24]. From Figure 4 it can be seen that ΔR_H at room temperature is about 0.6 times its value at 4.2°K, and if we assume a constant $R_{H,1}$ then σ_2/σ_1 has increased to 0.35 and

$\mu_{H,l}$ has only dropped to 36 cm^2/v-sec. While this value might seem a little high, especially for a more metal-rich composition, it is interesting to note that the room temperature mobility of pure palladium is about 7 cm^2/v-sec[25].

Thus it appears that the experimental results interpreted in terms of this model suggest that one of the phases in the palladium-silicon system near the 20 at.% silicon composition will display a somewhat high mobility for a metal, especially when the defects that are keeping its residual resistance ratio as high as 0.7 or more in the present case are eliminated. The only apparent alternative -- that the Hall coefficient is very sensitive to a general order that is not detectable to X-rays and barely noticeable in the resistivity -- would seem to be much less acceptable.

REFERENCES

(1)   W. Klement, R. H. Willens and Pol Duwez, Nature, 187, 869-870, (1960).

(2)   Pol Duwez, R. H. Willens and R. C. Crewdson, J. Appl. Phys., 36, 2267-2269, (1965).

(3)   R. C. Crewdson, Ph. D. Thesis, California Institute of Technology, (1966).

(4)   P. Pietrokowsky, Rev. Sci. Instr., 34, 445-446, (1963).

(5)   C. C. Chao, Ph. D. Thesis, California Institute of Technology, (1966).

(6)   H. Plate, Phys. Kond. Mat., 4, 355-374, (1966).

(7)   Pol Duwez, private communication.

(8)   Anna Nylund, Acta Chem. Scand., 20, 2381-2386, (1966).

(9)   C. C. Bradley, T. E. Faber, E. G. Wilson and J. M. Ziman, Phil. Mag., 7, 865-887, (1962).

(10)   Lev D. Landau and E. M. Lifshitz, Electrodynamics of Continuous Media, (Pergmon Press), (1960).

(11)   S. R. Coriell and J. L. Jackson, J. Appl. Phys., 39, 4733-736, (1968).

(12)   Charles Kittel, Introduction to Solid State Physics, (John Wiley and Sons, Inc., 2nd ed.), (1956).

(13)   James Clerk Maxwell, A Treatise on Electricity and Magnetism, (Dover Publications Inc., unabridged 3rd ed.), (1954).

(14) J. A. Reynolds and J. M. Hough, Proc. Phys. Soc. (London), B70, 769-775, (1957).

(15) J. W. S. Rayleigh, Phil. Mag., 34, 481-502, (1892).

(16) P. P. Ewald, Ann. Phys., 64, 253, (1921).

(17) J. Korringa, Physica, 13, 392, (1947).

(18) D.A.G. Bruggeman, Ann. Phys., 24, 636-664, (1935).

(19) D. J. Huntley, Can. J. Phys., 44, 2952-2956, (1966).

(20) K. S. Cole, C. L. Li and A. F. Bak, Exper. Neur., 24, 459-473, (1969).

(21) R. W. Sillars, J. Inst. Elect. Engrs., 80, 378-395, (1937).

(22) H. Juretschke, R. Landauer and J. A. Swanson, J. Appl. Phys., 31, 1939-1953, (1960).

(23) Conyers Herring, J. Appl. Phys., 31, 1939-1953, (1960).

(24) M. P. Lepselter and J. M. Andrews, in Ohmic Contacts to Semiconductors (Bertram Schwartz, ed.), (The Electrochemical Society, Inc.), 159-186, (1969).

(25) E. M. Savitskii, Palladium Alloys, (Primary Sources/Publishers), (1969).